Cell Reports, Volume *30*

Supplemental Information

Hypoxia Produces Pro-arrhythmic Late Sodium Current in Cardiac Myocytes by SUMOylation of $Na_V1.5$ Channels

Leigh D. Plant, Dazhi Xiong, Jesus Romero, Hui Dai, and Steve A.N. Goldstein

SUPPLEMENTAL TABLES

SUPPLEMENTAL FIGURES

Table S1. Biophysical parameters for mTFP-$Na_V1.5$ variants. Related to Figure 2.

Channel variant	I_{PEAK}, 21% O_2 pA/pF	I_{LATE}, 21% O_2 pA/pF	I_{PEAK}, 1.5% O_2 pA/pF	I_{LATE}, 1.5% O_2 pA/pF
mTFP-$Na_V1.5$	-198 ± 6	-0.96 ± 0.2	-201 ± 4	-8.3 ± 0.6
mTFP-$Na_V1.5$-K442Q	-200 ± 4	-0.93 ± 0.3	-197 ± 6	-0.91 ± 0.4*
mTFP-$Na_V1.5$-K496Q	-198 ± 3	-0.94 ± 0.2	-197 ± 3	-8.3 ± 0.3
mTFP-$Na_V1.5$-K1120Q	-193 ± 4	-0.95 ± 0.2	-196 ± 3	-8.7 ± 0.3
mTFP-$Na_V1.5$-K1162Q	-199 ± 4	-0.91 ± 0.2	-194 ± 5	-8.7 ± 0.4
mTFP-$Na_V1.5$-K1800Q	-195 ± 3	-0.97 ± 0.3	-193 ± 4	-8.8 ± 0.5

Legend. Human $Na_V1.5$ tagged with mTFP1 was expressed with $Na_V\beta1$ and studied in live CHO-K1 cells. As observed with untagged channels, mTFP-$Na_V1.5$-K442Q channels are insensitive to acute hypoxia. The effect of 1.5% O_2 on the magnitude of the peak (I_{PEAK}) and late (I_{LATE}) sodium current was assessed at -30 mV, as described in **Fig. 3.** Data are mean ± s.e.m. for 8 – 12 cells per group. Statistical significance between the condition studied and the normoxic condition for each cell was determined using a unpaired t-test, where $P<0.05$ is represented by an asterisk (*).

Table S2. Hypoxia-induced changes in I_{LATE} correlate with SUMOylation. Related to Figure 4.

Time after start of hypoxia, s	I_{LATE} (% I_{PEAK})	Manders' coefficient	Pearson's correlation coefficient
0	0.05 ± 0.07	0.10 ± 0.01	0.075 ± 0.01
50	2.8 ± 0.30	0.66 ± 0.02	0.62 ± 0.02
100	4.1 ± 0.44	0.91 ± 0.03	0.89 ± 0.015
300	4.0 ± 0.50	0.88 ± 0.03	0.86 ± 0.02
500	4.3 ± 0.49	0.89 ± 0.02	0.87 ± 0.03

Legend. The late current was determined as the %-change in peak current as per **Fig 5** and **Table 2** for $Na_V1.5$ channels expressed in CHO cells and studied in whole-cell mode. Briefly, cells were subject to hypoxia (1.5% O_2 at time = 0 s), and returned to 21% oxygen at 300 s; cells were studied for up to a total of 500 s. Manders' coefficient and Pearson's correlation coefficient were determined for the hypoxia-induced co-localization of mTFP-tagged $Na_V1.5$ channels and mCherry-tagged SUMO1 in TIRFM studies, as described in **Fig 4** using the Coloc2 algorithm in FIJI (ImageJ). Data are mean ± S.E.M. from 7-10 regions studied in 8 cells.

Table S3. Hypoxia yields a SUMO-dependent increase in APD in iPS-CMs. Related to Figure 5.

Parameter	Control			SUMO1			SENP1		
	21% O_2	1.5% O_2	1.5% O_2 + ranolazine	21% O_2	1.5% O_2	1.5% O_2 + ranolazine	21% O_2	1.5% O_2	1.5% O_2 + ranolazine
Resting potential, mV	-60.2 ± 3	-59.5 ± 3	-59.7 ± 3	-58.8 ± 2	-58.2 ± 3	-58.5 ± 3	-60.0 ± 1	-61.5 ± 4	-61 ± 2
dV/dt, V/s	15.4 ± 2	16.1 ± 3	15.8 ± 3	16.1 ± 2	15.8 ± 3	16.5 ± 1	16.6 ± 2	15.9 ± 4	15.5 ± 3
AP peak, mV	49.8 ± 3	50.5 ± 4	50.3 ± 3	51.2 ± 3	51.8 ± 4	51.5 ± 2	50 ± 3	48.5 ± 1	49 ± 2
APD_{50}, ms	663 ± 28	810 ± 19*	690 ± 17	822 ± 22	869 ± 27	699 ± 20*	663 ± 26	699 ± 24	663 ± 19
APD_{90}, ms	918 ± 32	1122 ± 26*	945 ± 28	1127 ± 24	1184 ± 27	905.4 ± 30*	909 ± 32	947 ± 21	905.4 ± 29

Legend. Human cardiac myocytes derived from iPS cells (**Fig. 1 & 5**) were studied by current-clamp in whole-cell mode. Spontaneous action potentials were studied with control intracellular solution of with 1 nM SUMO1 or SENP1 in the recording pipette with the same sequence of perfusates: normoxic (21% O_2), hypoxic (1.5% O_2), then hypoxia with 1 μM ranolazine. dV/dt is the velocity of the upstroke of the action potential. The action potential duration (APD_{50} and APD_{90}) was determined by calculating the time required for the membrane potential to return to 50% and 90% of the resting value from the peak deflection of the action potential. Data are means ± S.E.M. for 6-9 cells studied per group; statistical significance between the condition studied and the normoxic condition for each cell was determined using a two-way paired t-test, * indicates $P<0.01$.

Figure S1. Hypoxia, or SUMO1 in ambient oxygen, augment $Na_V1.5$ window-current in human iPS-CMs. Related to Figure 1.

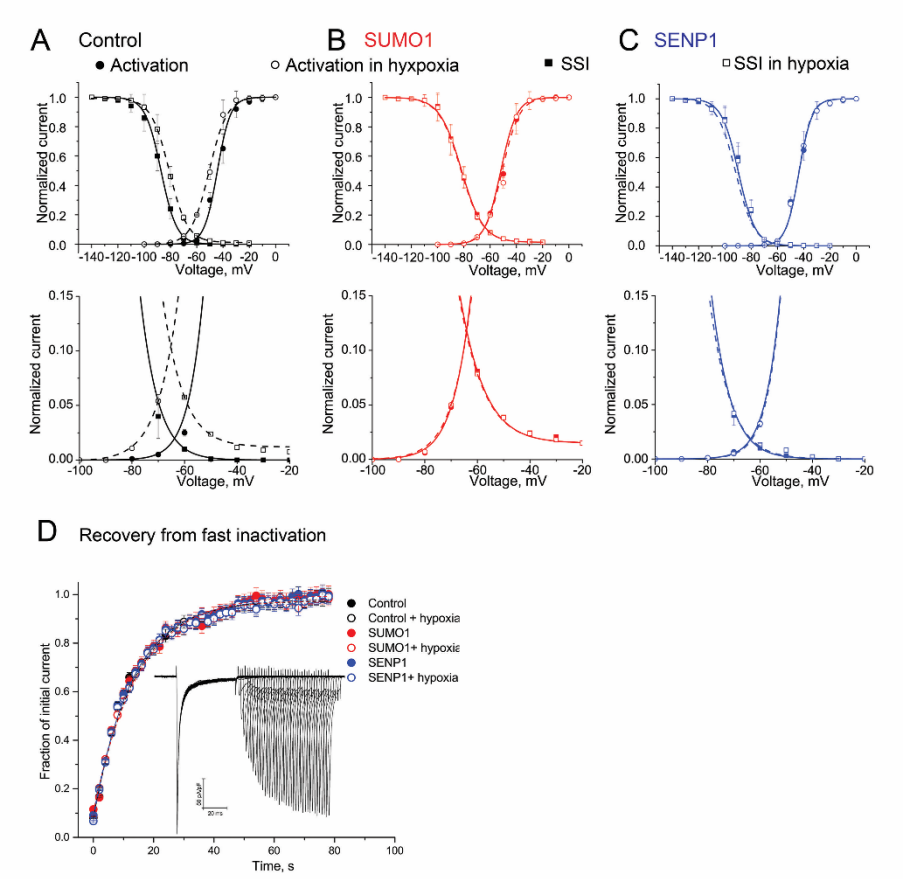

Legend. I_{LATE} is observed in the 'window' between the voltages where Na_V channels activate and inactivate. The window-current in iPS-CMs was studied by measuring the voltage-dependence of I_{Na} activation (circles) and steady-state inactivation (SSI, squares). Activation was assessed using current-voltage relationships evoked from a holding potential of -100 mV by 100 ms test pulses between -100 and 0 mV, in 10 mV increments. Steady-state inactivation was studied by holding cells at -140 mV and then comparing currents evoked by 50 ms test pulses between -140 mV and -20 mV to those evoked by a 100 ms prepulse to 0 ms. A 10 s interpulse interval was used in both cases. Normalized peak currents were plotted against prepulse potential (mV). Normalized activation and inactivation relationships were fit with a Boltzmann function, $I = Imax/(1 + \exp[V - V½/k])$, where *Imax* is the maximum current and *k* is slope factor. Data are mean ± S.E.M. for 8 to 10 cells per group.

A. *Upper*, when cells were studied with a control pipette solution, exchanging the normoxic perfusate (**black line**) with a hypoxic perfusate (**black dash**) left shifted the V½ of activation and right shifted V½-SSI. *Lower*, the changes in activation and SSI increased the magnitude of the window current.

B. *Upper*, when cells were studied with 1 nM SUMO1 in the pipette (**red line**) the V½-activation was left shifted compared to control (**A**) and V½-SSI was right shifted. The currents were insensitive to hypoxia (**red dash**). *Lower*, SUMO1 increased the magnitude of the window current compared to control (**A**).

C. *Upper*, 1 nM SENP1 in the pipette (**blue line**) did not alter the V½ of activation or SSI compared to control (**A**) and currents were insensitive to hypoxia (**blue dash**). *Lower*, SENP1 did not change the window current.

D. The recovery of I_{Na} from fast inactivation is not altered by hypoxia, SUMO1 or SENP1. The rate at which I_{Na} recovered from fast inactivation was determined using the protocol detailed in the methods. The time-constant for recovery τ, was obtained by fitting the normalized current amplitude to the recovery time using the mono-exponential function: $I_t = I_{max} + A\left[e^{-t/\tau}\right]$. The mean τ ± s.e.m. was not different for 6-8 cells

studied under each of the experimental conditions indicated. For iPS-CMs studied with control pipette solution, τ was 13.6 ± 0.6 ms under ambient conditions and 12.9 ± 0.3 ms when the cells were subjected to hypoxia. The exemplar record, inset, shows the recovery of $Na_V1.5$ channels studied in ambient levels of O_2. When cells were studied with 1 nM SUMO1 in the pipette, τ was 14.8 ± 1 ms in normoxia and 13.7 ± 0.8 ms in hypoxia. When 1 nM SENP1 was included in the pipette, τ changed from 13.2 ± 0.3 ms in normoxia and 12.4 ± 0.5 ms in hypoxia. Similar results were obtained for $Na_V1.5$ and $Na_V1.5$-K442Q channels expressed in CHO-K1 cells with $Na_V\beta1$.

Figure S2. FRET shows SUMOylation of $Na_V1.5$ K442 and no other site. Related to Figure 2.

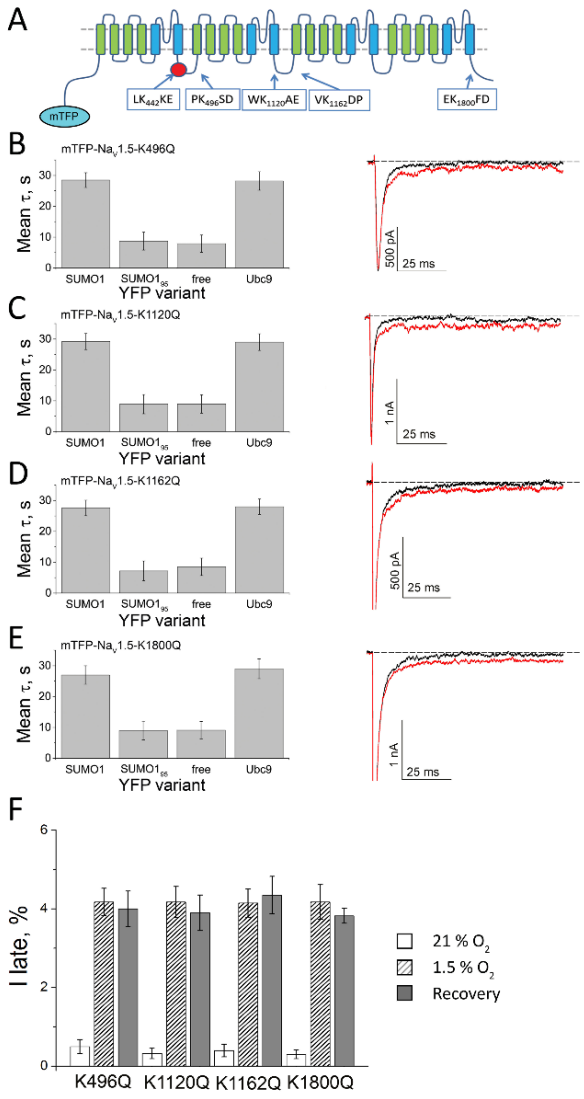

Legend. Human $Na_V1.5$ tagged with mTFP1 was expressed with $Na_V\beta1$ and studied in live CHO-K1 cells. FRET between mTFP1 (donor) and YFP-tagged subunits (acceptor) was assessed by donor photobleaching, as described in **Fig. 2**. Data are mean τ ± s.e.m. for 3 regions of 5-7 cells per group. The effect of 1.5% O_2 on the magnitude of the late sodium current was assessed at -30 mV, as described in **Fig. 3.**

A. A cartoon showing the secondary structure of mTFP-$Na_V1.5$ and the location of putative SUMOylation sites identified by the SUMOplot algorithm. K442, the only site where SUMO1 was found to interact with $Na_V1.5$ (**Figs. 2-4**) is in red.

B. *Left*, A histogram of mean FRET τ–values show assembly of mTFP-$Na_V1.5$-K496Q channels with YFP-SUMO1 and YFP-Ubc9 but not linkage-incompetent YFP-$SUMO1_{95}$ or free YFP. *Right*, Exemplar currents show the development of late current when cells expressing mTFP-$Na_V1.5$-K496Q were studied in ambient (black) and hypoxic conditions (red).

C. **E.** FRET studies show that mTFP- $Na_V1.5$-K1120Q, mTFP- $Na_V1.5$-K1162Q and mTFP- $Na_V1.5$-K1800Q channels interact with YFP-SUMO1 and Ubc9 like wild type and whole-cell current recording shows that hypoxia induced I_{LATE} in each of the channels.

F. A histogram showing the mean I_{LATE} as % of peak current from cells studied at 21% O_2 (open), after 200 s at 1.5% O_2 (hatched) and after 200 s following a return to 21% O_2 with the pipette solutions indicated (grey).

Figure S3. Acute hypoxia and SUMO1 augment the $Na_V1.5$ channel window current in CHO cells. Related to Figure 3.

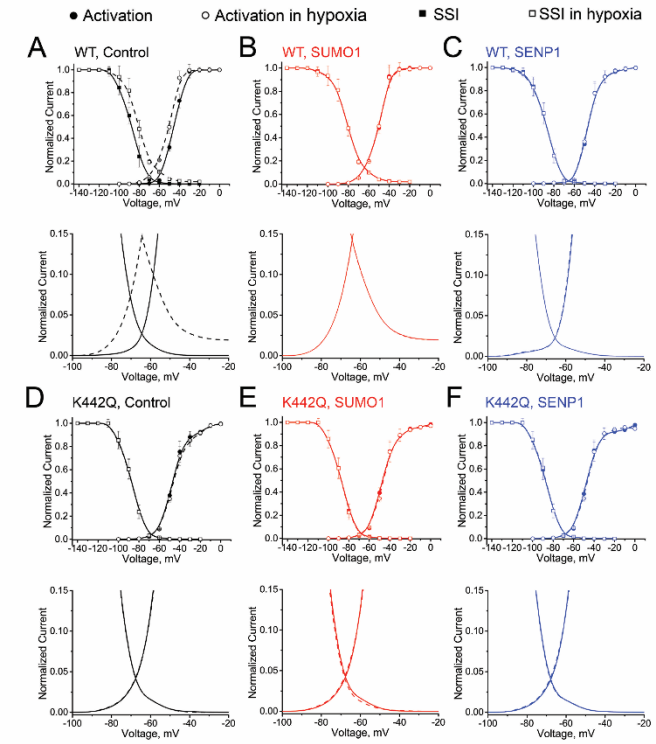

Legend. $Na_V1.5$ or $Na_V1.5$-K442Q were express in CHO-K1 cells with $Na_V\beta1$ and studied in whole-cell mode to determine normalized activation (circles) and steady-state inactivation (SSI; squares) relationships for peak currents, as described in the STAR Methods and for iPS-CMs in **Fig. S1**. Measured values are noted in the text and **Table 1**. Hypoxia was 1.5% O_2. Cells were studied with control solution (**black**), 1 nM SUMO1 (**red**), or 1 nM SENP1 (**blue**) in the recording pipette. Data are mean ± S.E.M. for 8 to 10 cells per group.

A. *Upper*, when $Na_V1.5$ channels were studied with a control pipette solution, exchanging the normoxic perfusate (**black line**) with a hypoxic perfusate (**black dash**) left shifted the V½ of activation and right shifted V½-SSI. *Lower*, the changes in activation and SSI increased the magnitude of the window current.

B. *Upper*, studying $Na_V1.5$ channels with 1 nM SUMO1 in the pipette (**red line**) left-shifted the V½-activation compared to control (**A**) and right shifted V½-SSI. The currents were insensitive to hypoxia (**red dash**). *Lower*, SUMO1 increased the magnitude of the window current compared to control (**A**).

C. *Upper*, 1 nM SENP1 in the pipette (**blue line**) did not alter the V½ of activation or SSI compared to control (**A**) and the currents were insensitive to hypoxia (**blue dash**). *Lower*, SENP1 did not change the window current.

D. **F.** The V½-act and the V½-SSI of cells expressing $Na_V1.5$-K44Q was not altered by hypoxia, or when the cells were studied with 1 nM SUMO1 or SENP1 in the recording pipette.

Figure S4. Mass spectroscopic demonstration of SUMOylation of $Na_v1.5$ K442. Related to Figures 2 and 3.

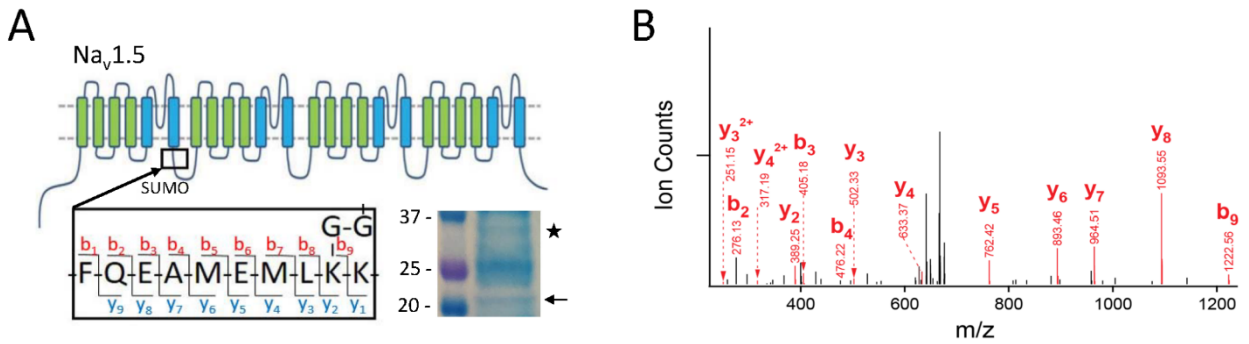

Legend. For MS analysis, $Na_V1.5_{353-502}$ and $SUMO1_{97}T95K$ were expressed with SUMOylation enzymes in *E. coli*, purified, subjected to trypsin cleavage, and analyzed by MS as in the STAR Methods.

A. *Top,* schematic showing the product $Na_V1.5_{353-502}$-SUMO (box) and the trypsin fragment of $Na_V1.5$ carrying the Gly-Gly remnant of $SUMO1_{97}T95K$. *Bottom left,* the sequence of the three-ended fragment with K442 and the Gly-Gly remnant. *Bottom right,* a Coomassie blue-stained SDS-PAGE gel of the purified products. Unmodified $Na_V1.5_{353-502}$ migrates at ~20 kDa (arrow). Expression of $SUMO1_{97}T95K$ (SUMO) and the SUMO enzymes yields SUMO on the overexpressed target as well as native protein and the $Na_V1.5_{353-502}$-SUMO conjugate migrates at ~ 35 kDa (star). Molecular weight markers are shown.

B. Tandem MS sequence analysis of the fragment with Lys442 and the Gly-Gly remnant indicating *b* and *y* ion species as annotated in (a).

Figure S5. Reopening of single $Na_V1.5$ channels requires SUMO1. Related to Figure 3.

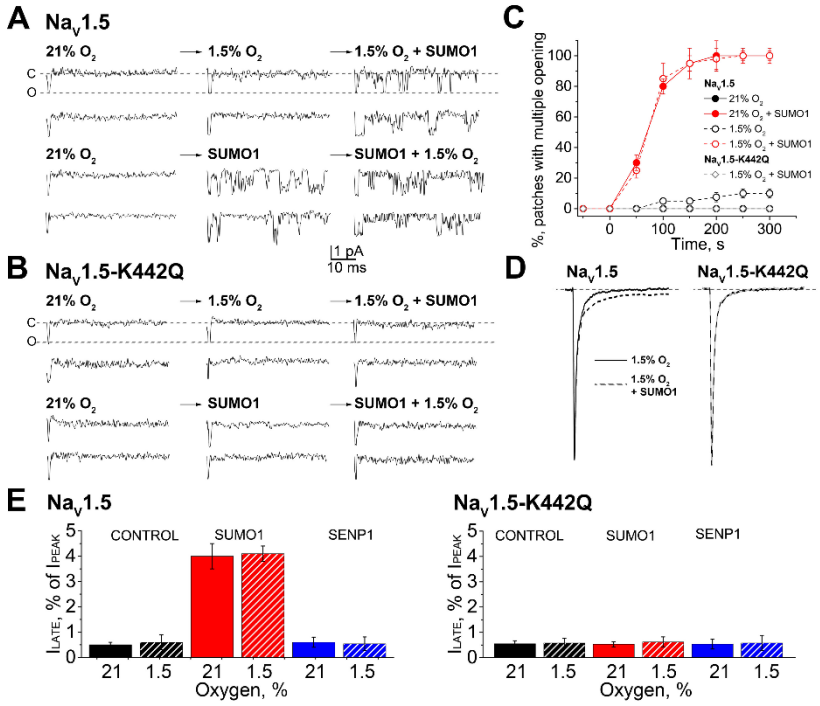

Legend. Human $Na_V1.5$ and $Na_V\beta1$ were studied in inside-out patches excised from CHO-K1 cells, as described in the STAR Methods. Single-channel currents were stimulated every 5 s by a 50-ms depolarizing pulse to –30 mV from a holding potential of –120 mV. Data were recorded at filter and sampling frequencies of 5 and 50 kHz, respectively but were refiltered offline using a 1 kHz Bessel filter for display purposes. For each cell, null sweeps (with no channel activity) were identified, averaged offline, and subtracted from data sweeps before analysis. Recording pipettes were filled with extracellular buffer and the inside of patches was perfused with the intracellular buffer, with or without 1 nM SUMO1 or 1 nM SENP1, as indicated. Hypoxia, 1.5% O_2.

A. Upon depolarization, single $Na_V1.5$ channels opened, inactivated rapidly, and did not reopen when studied in normoxia or when exposed to hypoxia. The addition of 1 nM SUMO1 induced channel reopening in patches studied in 1.5% O_2 (*upper*), or 21% O_2 (*lower*). Null traces were 50 ± 4% (n = 10 patches; 1,000 sweeps) for both configurations of the experiment.

B. Upon depolarization, single $Na_V1.5$-K442Q channels opened, inactivated rapidly, and did not reopen when exposed to hypoxia or 1 nM SUMO1. Null traces were 52 ± 6% (n = 10 patches; 1,000 sweeps) for both configurations of the experiment.

C. A scatter plot showing the portion of patches with single $Na_V1.5$ channels that that showed reopening plotted against time after the transition to hypoxia. $Na_V1.5$ channels were studied in 21% O_2 (●), 21% O_2 + SUMO1 (●), 1.5% O_2 (O), 1.5% O_2 + SUMO1 (O). Reopening was observed with SUMO1 in both 21% and 1.5% O_2, reached at maximum at 155 ± 7 s in each case, with 50% of the patches showing channel reopening at 65 ± 10 s and 67 ± 8 s respectively. $Na_V1.5$-K442Q channels were studied with 1.5% O_2 + SUMO1 (◇) and did not reopen.

D. Ensemble average traces (n = 200-220 sweeps per channel) showing that hypoxia-induced reopening of $Na_V1.5$ channels leads to I_{LATE} only in the presence of SUMO1.

E. *Left,* A histogram showing the mean I_{LATE} as a % of the peak current from ensemble average currents obtained from off-cell patches studied at 21% O_2, and after 200 s at 1.5% O_2 with the intracellular solutions indicated. *Right,* A histogram showing the mean I_{LATE} as a % of the peak current from ensemble average currents obtained from off-cell patches studied at 21% O_2, and after 200 s at 1.5% O_2 with the intracellular solutions indicated.

Figure S6. Hypoxia does not recruit SUMO1 to $Na_V1.5$-K442Q channels at the cell surface.

Related to Figure 4.

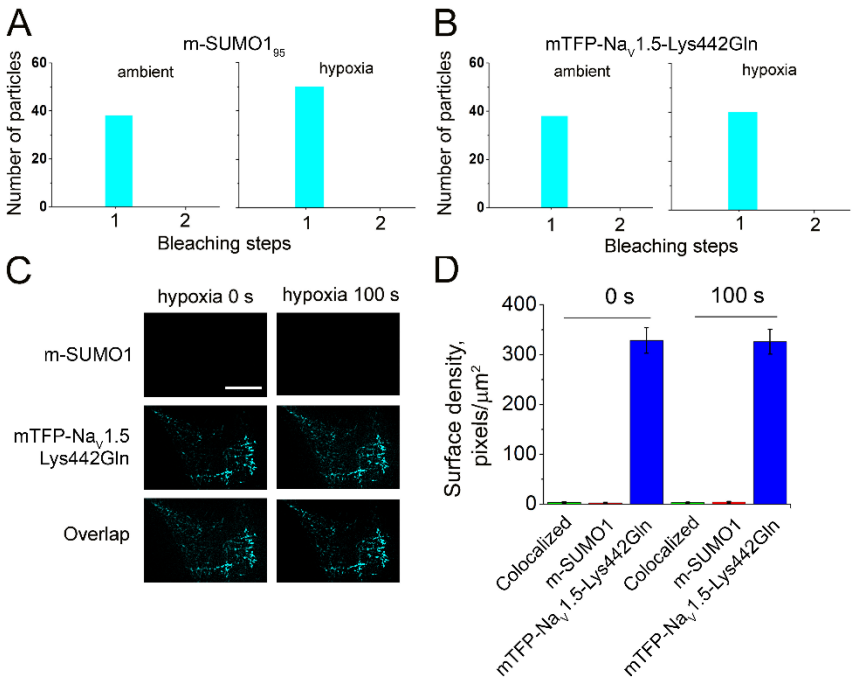

Legend. Single mTFP-$Na_V1.5$ and mTFP-$Na_V1.5$-K442Q channels and mCherry-SUMO1 (m-SUMO1) were studied in CHO-K1 cells by TIRFM. Stoichiometric (photobleaching) and pixel-by-pixel analysis for subunit density and colocalization were studied as per **Fig. 4**. The surface-density of fluorescent pixels was assessed post-hoc for 3–5 regions per cell. Stoichiometric analysis represents 5–8 cells and is summarized in **Table 2**.

A. Histogram of photobleaching steps showing that m-SUMO1$_{95}$, lacking the C-terminal diglycine motif required for conjugation is not observed at the cells surface, despite the expression of mTFP-$Na_V1.5$ channels (teal, single bleaching step per particle). Hypoxia does not increase the surface presence of m-SUMO1$_{95}$ and does not alter the channel subunit stoichiometry (**Table 2**).

B. Histogram of photobleaching steps showing that mTFP-$Na_V1.5$-K442Q channels contain one subunit in normoxic and hypoxia conditions and do not associate with m-SUMO1.

C. *Left*, in ambient O_2 (0 seconds of hypoxia), the surface density of m-SUMO1 (top) is low compared to mTFP-$Na_V1.5$-K442Q channels (middle) with little co-localization (bottom). *Right*, hypoxia does not recruit m-SUMO1 to the cell surface and m-SUMO1 is not observed to colocalize with mTFP-$Na_V1.5$-K442Q channels (bottom); surface levels of mTFP-$Na_V1.5$-K442Q were not observed to change (middle).

D. Histogram of surface density summarizing six cells studied as described in (**A**) and **Table 2**. At ambient O_2 (0 seconds of hypoxia), the density of pixels per µm^2 with SUMO1 alone (red) was 2.8 ± 1.0, and 328 ± 26 for $Na_V1.5$-K442Q (blue). The density of pixels with both fluors was 3.6 ± 1 per µm^2 (green). This distribution of subunits was not altered by 100 s hypoxia. Cells were observed to have 3.3 ± 1 colocalized pixels per µm^2, 326 ± 25 pixels with free $Na_V1.5$ channels per µm^2 and 4 ± 2 pixels per µm^2 with free SUMO1.